

AD-A271 196

TION PAGE

Form Approved  
OMB No. 0704-0188



Average 1 hour per response, including the time for reviewing instructions, searching existing data sources, the collection of information. Send comments regarding this burden estimate or any other aspect of this Washington Headquarters Service, Directorate for Information Operations and Reports, 1215 Jefferson Management and Budget, Paperwork Reduction Project (0704-0188), Washington, DC 20543.

23

4. REPORT DATE 07/31/93		3. REPORT TYPE AND DATES COVERED Technical 06/01/93 - 05/31/94	
4. TITLE AND SUBTITLE Cooperative Formation of Inorganic-Organic Interfaces in the Synthesis of Silicate Mesostructures		5. FUNDING NUMBERS N00014-90-J-1159	
6. AUTHOR(S) A. Monnier, F. Schuth, Q. Huo, D. Kumar, D. Margolese, G.D. Stucky, M. Krishnamurty, P. Petroff, A. Firouzi, M. Janicke, B.F. Chmelka		8. PERFORMING ORGANIZATION REPORT NUMBER T1	
7. PERFORMING ORGANIZATION NAME(S) AND ADDRESS(ES) University of California Department of Chemistry Santa Barbara, CA 93106			
9. SPONSORING/MONITORING AGENCY NAME(S) AND ADDRESS(ES) Office of Naval Research Chemistry Program 800 N. Quincy Street Alexandria, VA 22217		10. SPONSORING/MONITORING AGENCY REPORT NUMBER	
11. SUPPLEMENTARY NOTES Prepared for Publication in Science (Accepted)			
12a. DISTRIBUTION/AVAILABILITY STATEMENT Approved for public release; distribution unlimited			
13. ABSTRACT (Maximum 200 words) A model is presented to explain the formation and morphologies of surfactant-silicate mesostructures. Three processes are identified: multidentate binding of silicate oligomers to the cationic surfactant; preferential silicate polymerization in the interface region; and charge density matching between the surfactant and the silicate. The model explains present experimental data, including the transformation between lamellar and hexagonal mesophases, and provides a guide for predicting conditions favoring the formation of lamellar, hexagonal or cubic mesostructures. The model Q <sup>230</sup> proposed by Mariani <i>et al.</i> (21) satisfactorily fits the X-ray data collected on the cubic mesostructure material. This model suggests that the silicate polymer forms an unique infinite silicate sheet sitting on the gyroid minimal surface and separating the surfactant molecules into two disconnected volumes.			
14. SUBJECT TERMS		15. NUMBER OF PAGES 25	
		16. PRICE CODE	
17. SECURITY CLASSIFICATION OF REPORT Unclassified	18. SECURITY CLASSIFICATION OF THIS PAGE Unclassified	19. SECURITY CLASSIFICATION OF ABSTRACT Unclassified	20. LIMITATION OF ABSTRACT UL

93 10 18 064

93-24766



## Cooperative Formation of Inorganic-Organic Interfaces in the Synthesis of Silicate Mesostructures

A. Monnier<sup>1,4</sup>, F. Schüth<sup>1,5</sup>, Q. Huo<sup>1</sup>, D. Kumar<sup>1</sup>, D. Margolese<sup>1</sup>, R. S. Maxwell<sup>1</sup>, G. D. Stucky<sup>1\*</sup>,  
M. Krishnamurthy<sup>2</sup>, P. Petroff<sup>2</sup>, A. Firouzi<sup>3</sup>, M. Janicke<sup>3</sup>, B. F. Chmelka<sup>3</sup>

<sup>1</sup>Department of Chemistry

<sup>2</sup>Materials Department

<sup>3</sup>Department of Chemical and Nuclear Engineering  
University of California, Santa Barbara, CA 93106

<sup>4</sup>Departement de Chimie Physique  
Sciences II, 1211 Geneva, Switzerland

<sup>5</sup>Institut für Anorganische Chemie  
Johannes-Gutenberg-Universität, 6500 Mainz, Germany

**Abstract**

A model is presented to explain the formation and morphologies of surfactant-silicate mesostructures. Three processes are identified: multidentate binding of silicate oligomers to the cationic surfactant; preferential silicate polymerization in the interface region; and charge density matching between the surfactant and the silicate. The model explains present experimental data, including the transformation between lamellar and hexagonal mesophases, and provides a guide for predicting conditions favoring the formation of lamellar, hexagonal, or cubic mesostructures. The model Q<sup>230</sup> proposed by Mariani and coworkers satisfactorily fits the X-ray data collected on the cubic mesostructure material. This model suggests that the silicate polymer forms an unique infinite silicate sheet sitting on the gyroid minimal surface and separating the surfactant molecules into two disconnected volumes.

Accession For	
NTIS CRA&I	<input checked="" type="checkbox"/>
DTIC TAB	<input type="checkbox"/>
Unannounced	<input type="checkbox"/>
Justification	
By .....	
Distribution/	
Availability Codes	
Dist	Avail and/or Special
A-1	1/2/80

The invention of a new family of mesoporous silica materials, designated M41S, by scientists at Mobil Oil Corp. (1), has dramatically expanded the range of crystallographically defined pore sizes from the micropore ( $<13 \text{ \AA}$ ) to the mesopore (20-100  $\text{\AA}$ ) regime. The synthesis uses ordered arrays of surfactant molecules as a "template" for the three-dimensional polymerization of silicates. The mesoporous materials obtained by this route exhibit several remarkable features: i) well defined pore sizes and shape, as compared to other mesoporous materials; ii) fine adjustability of the pore size within the limits stated above; iii) high thermal and hydrolytic stability if properly prepared; and iv) a very high degree of pore ordering over micron length scales. These important and unusual properties are a direct result of the interplay between organized arrays of the surfactant molecules and silicate species in the aqueous phase.

Beck *et al.* (2) outlined two general pathways for the formation of the mesoporous silicates. The first model assumes that the primary structure-directing element is the water-surfactant liquid crystal phase. The second model suggests that the addition of the silicate produces the ordering of the subsequent silicate-encased surfactant micelles. These general models, however, are insufficient for establishing the mechanistic understanding needed for better control of the synthesis process. Such understanding is key to efforts aimed at improving or adding to this exciting new class of materials. Based on new experimental results, we present here a more detailed model of the mesophase formation process, which explains presently known experimental data and successfully predicts conditions needed for the synthesis of desired structures. We believe that this model can be generalized to the synthesis of other non-siliceous materials as well.

From considerations in surfactant and silicate chemistry, three closely coupled phenomena are identified as crucial to the formation of surfactant-silicate mesophases: i) multidentate binding of silicate oligomers; ii) preferred polymerization of silicates at the surfactant-silicate interface; and iii) charge density matching across the interface.

It is important to note that mesostructure syntheses can be carried out under conditions where the silicate alone would not condense (at pH's from 12-14 and silicate concentrations of 0.5-5%) and the surfactant cetyltrimethylammonium ( $\text{CTA}^+$ ) alone would not form a liquid crystal phase. In fact,

surfactant-silicate mesophases can form at surfactant concentrations as low as 1%, a regime in the CTABr-water phase diagram where only micelles are present. For a CTABr-water solution at typical surfactant-silicate synthesis temperatures in the absence of silicates, an hexagonal phase is favored at surfactant concentrations from ~25-70% by weight, while a lamellar phase forms at concentrations above 70% (3,4). Nevertheless, a solid mesophase precipitate is formed, the structure of which will be discussed below, as soon as surfactant (8 to 20 carbon chain length) and silicate solutions are combined. The rapidity of this precipitation indicates that a strong interaction between the cationic surfactant and anionic silicate species is involved in the formation of surfactant-silicate mesophases.

Syntheses aimed at identifying conditions important for the formation of mesoporous materials were performed over a wide range of reactant compositions and temperatures (5). For the purpose of investigation, evolution of the surfactant-silicate systems could be slowed by undertaking the syntheses at moderate temperatures between 30-100°C (6). During freeze-dry kinetic experiments using CTACl as the surfactant, a layered (lamellar) material with a primary  $d$ -spacing (i.e. repeat distance) of  $31(\pm 1)$  Å was produced, together with amorphous silica, after reaction times on the order of one minute. For the synthesis conditions given in Figure 1, the lamellar mesophase disappears after approximately 20 min, at which point the diffraction pattern of the hexagonal mesostructure is simultaneously detected. This hexagonal material has a primary  $d$ -spacing of  $40(\pm 1)$  Å and attains its final degree of ordering after ~10 hours (7).

A layered material with a primary  $d$ -spacing of  $31(\pm 1)$  Å (Fig. 2, pattern A) can be isolated in pure form (8); a transmission electron microscopy (TEM) micrograph of this mesostructure is depicted in Figure 3. The variation of the  $d$ -spacing as a function of the chain length of a cationic surfactant  $C_nH_{2n+1}[N(CH_3)_3]^+$  (for  $14 \leq n \leq 22$ ) has been determined to be 1.0 to 1.2 Å/carbon, which corresponds to a monolayer assembly. If this new layered material is hydrothermally treated at 373 K (pH=7), it is converted to the hexagonal mesostructure over 10 days, with intermediate and final X-ray patterns shown in Figure 2(b,c). During this transformation the degree of silica polymerization increases, based on the relative amounts present of incompletely condensed ( $Q^3$ ) and fully condensed ( $Q^4$ ) silicon atoms measured using  $^{29}\text{Si}$  magic-angle spinning nuclear magnetic resonance

spectroscopy (NMR). The ratio between Q<sup>3</sup> and Q<sup>4</sup> silicon decreases as a function of time from typical values of 1.0 for the layered material to 0.4 - 0.55 for the hexagonal mesostructure, reflecting a significant increase in the number of silicon atoms fully coordinated to other silicate nearest neighbors.

Mesophase formation and associated silica polymerization are tied intimately to Coulombic interactions between surfactant and silicate species at the micelle interfaces. Silicates present in the form of monovalent monomers, Si(OH)<sub>3</sub>O<sup>-</sup>, however, are expected to have little energetic advantage over other monovalent anions competing for access to the cationic surfactant head groups. At high pH, the reaction mixture also contains small silica oligomers (3-7 Si atoms) of varying degrees of polymerization and charge (9). These oligomers are appreciably more acidic [pK<sub>a</sub> ~6.5] than the monomer or dimer species [pK<sub>a</sub> 9.8 and 10.7, respectively (10)], though all such silicates will be highly dissociated under the high pH conditions employed here (11). The oligomeric silica polyanions, however, can easily act as multidentate ligands for the cationic head groups of the surfactant, leading to a strongly interacting surfactant-silicate interface. Indeed, the interaction of ionic surfactants with polyions of opposite charge is known to encourage strong cooperative binding, manifested by increases in the binding constants of up to two orders of magnitude in similar systems (12). Preferential multidentate binding of the silicate polyanions results in the interface being quickly populated by tightly held silicate oligomers, which can subsequently polymerize further. Silicate polymerization within the surfactant-silicate interface region is favorable for two related reasons: i) the concentration of silicate species near the interface is high; and ii) their negative charges are partially screened by the surfactant. Furthermore, as polymerization proceeds, the formation of highly connected silicate polyanions, which act as very large multidentate ligands, further enhances the cooperative binding between the surfactant and silicate species.

Multidentate ionic binding in surfactant-silicate systems has an important consequence, namely it leads to precipitation of a given mesophase from solution. Through the interactions driving the precipitation process, the appearance of a given mesostructure is established, though this is expected to operate on a different time scale from polymerization of the silica, which accounts ultimately for the thermal, mechanical, and hydrolytic stability of the final material. Provided small silica oligomers are

present in sufficient quantity, precipitation of the surfactant-silicate system is primarily the result of electrostatic interactions, combined with packing constraints associated with the hydrophobic surfactant chains. Whereas precipitation is fast and essentially thermodynamically controlled, silica polymerization into a strong and extended framework is slow and reaction rate limited. This two-stage process is in agreement with experimental findings that contrast the mesostructures obtained at room temperature after short reaction time with those obtained at high temperature after long reaction time: very similar X-ray patterns are obtained for both sets of conditions indicating identical precipitated mesostructures, however, the materials synthesized by the low temperature route are thermally and mechanically much less stable when compared to the high temperature analogues. The coupling between the precipitation and polymerization processes in surfactant-silicate systems provides the basis for the lamellar-to-hexagonal mesophase transformation in a way that we now describe.

The resemblance, in shape and size, of the surfactant-silicate mesostructures with the corresponding water-surfactant liquid crystal phases indicates that the interactions responsible for these morphologies are of a similar nature. The governing role of the head-group area ( $A$ ) in the selection of a particular mesophase has already been recognized in water-surfactant systems: the favored mesophase is that which permits the head-group area  $A$  to be closest to its optimal value  $A_0$ , while maintaining favorable packing of the hydrophobic surfactant chains (13). In surfactant-silicate systems, the value of  $A_0$  is strongly affected by electrostatic and steric interactions between the silicate and surfactant micelle species. More quantitatively, its value is obtained by minimizing the Gibbs free energy  $G$  as a function of head-group area  $A$ :

$$A_0 \Rightarrow (\partial G / \partial A) = 0 \quad , \quad (1)$$

$$G(A, \rho) = G_{\text{intra}}(A) + G_{\text{wall}}(\rho) + G_{\text{inter}}(A, \rho) + G_{\text{sol}} \quad , \quad (2)$$

where  $G_{\text{intra}}$  reflects the van der Waals forces and conformational energy of the hydrocarbon chains and van der Waals and electrostatic interactions of the head group within a single micelle;  $G_{\text{wall}}$

accounts for the polysilicate structural free energy, including the solvent, counterion, and silicate van der Waals and electrostatic interactions within the inorganic silicate framework or "wall";  $G_{\text{inter}}$  reflects the van der Waals and electrostatic effects associated with wall-micelle and micelle-micelle interactions;  $G_{\text{sol}}$  describes the solution phase; and  $\rho$  specifies the composition of the various species within the wall. The chemical potentials of these species are set by the concentration of the corresponding species in the aqueous solution, as accounted for by  $G_{\text{sol}}$ .

Physically,  $G_{\text{intra}}$  governs the formation of a particular micelle shape for a given head-group area  $A$  and is also responsible for the observed swelling of the micelles when hydrocarbon "expanders", such as trimethylbenzene (TMB) are added to the solution (14). The term  $G_{\text{wall}}$  drives the chemistry within the wall, including the polymerization process, and contains the structural constraints responsible for the multidentate binding.  $G_{\text{inter}}$  establishes the relationship between the head-group area  $A$  and the state of the wall described by  $\rho$ . This coupling across the interface can be understood in terms of electrostatic interactions (which most likely predominate), whereby the charge density within the wall  $\rho_E$ , is mutually screened by the charges on the surfactant head groups, which possess an average surface charge density  $1/A$ . Thus the electrostatic interactions link the optimal head-group area  $A_0$ , as defined by Equation 1, with the silicate charge density  $\rho_E$ , a relationship we refer to as "charge density matching." Such interdependent electrostatic effects have been previously shown to control the  $d$ -spacings of surfactant intercalates in different mica-type silicates (15), and also invoked to explain the "self-replication" process of silica layers in purely inorganic systems (16).

In surfactant-silicate systems, polymerization driven by  $G_{\text{wall}}$  will profoundly affect the wall charge density  $\rho_E$ , providing a mechanism to explain the transition between the lamellar and the hexagonal mesophases. In the early stage of the synthesis, the presence of highly charged silica oligomers favors a small head-group area  $A_0$ , which can be achieved with a lamellar surfactant configuration. As rearrangement and polymerization of the silicate species proceed, the density of anionic silanol groups diminishes, so that the optimal head-group area  $A_0$  increases, while the number of compensating cations decrease. At the same time, the wall thickness can decrease from its initial value without energy cost, because the most stable ionized silanol groups are confined to the wall



surface, thus reducing repulsive dipole-dipole interactions between the two opposite-facing wall surfaces. The silicate wall is still poorly condensed during early stages of the synthesis, allowing the system to increase its head-group area  $A$  toward  $A_0$  by adopting the hexagonal structure according to charge-density matching criteria. Under these circumstances, the wall thickness simultaneously decreases to keep the volume ratio  $\text{CTA}/\text{SiO}_2$  constant. The actual wall thickness has been estimated to be 10-11 Å (17) for the lamellar mesophase and 8-9 Å (18) for the hexagonal mesophase. These values are consistent with a constant  $\text{CTA}/\text{SiO}_2$  volume ratio throughout the phase transition using simple geometrical arguments.

The regularity of the product mesostructures supports mediation of the silicate wall thickness during the assembly process. The high efficiency of this mediation is reflected by the experimental observation that the wall thickness of the hexagonal phase is essentially constant (8-9 Å) over a wide range of reaction conditions, independent of the surfactant chain length, and by the clearly hexagonal, as opposed to circular, pore shape established by both high resolution TEM and modeling of the powder X-ray diffraction patterns (19). Control of the silicate wall thickness is undoubtedly related to the double layer potential: silicate species are only accumulated at the surfactant interface to the extent necessary for charge compensation. Polymerization normal to the interface, which would thicken the wall or produce amorphous bulk  $\text{SiO}_2$ , does not occur because of the strong electrostatic repulsion produced by the high negative charge on the silicate species at pH 12 and above (10).

Figure 4 shows a mechanism consistent with current experimental investigations by which the lamellar-to-hexagonal mesophase transformation may occur. Silica polymerization leads to an increase in interfacial area that is achieved through corrugation of the lamellar surfactant-silicate sheets. As implied in the final step, this corrugation progresses until connection between the sheets is made at the cusps, resulting ultimately in formation of the hexagonal mesophase. Note that another way to accommodate the change in head-group area  $A$  would be to maintain a planar structure while tilting the hydrocarbon chains. Such a transition however, is entropically disfavored by the restrictive chain configuration this suggests.

Yanagisawa *et al.* (20) recently reported an hexagonal mesostructure, with pore dimensions similar to that of M41S, produced by inclusion of  $\text{CTA}^+$  cations into the sheet silicate kanemite. During their synthesis the authors observed a layered intermediate that subsequently transformed into an hexagonal phase material. This process is probably driven by the same forces as the transformation we report, though it is not yet clear to what extent the kanemite structure is preserved during the conversion. If the pH is sufficiently basic, for example, the sheets can be partially or fully destroyed during the process.

We propose that the surfactant-silicate mesophase structure is governed primarily by the terms  $G_{\text{intra}}$  and  $G_{\text{inter}}$  of Equation 2. In this respect, the main effect of the silicate wall and of the reaction conditions are to determine the optimal head-group area  $A_0$ . This provides predictive capability for establishing the reaction conditions that favor the lamellar or the hexagonal mesophases. This model has been tested experimentally by monitoring the effects of pH and the degree of polymerization of the silica source on the mesostructure syntheses, with the results summarized in Figure 5. These lead to the following conclusions in accordance with our predictions:

- 1) The lamellar phase is favored at high pH and for a low degree of polymerization of the silica source.
- 2) The hexagonal phase is favored at low pH and for a highly polymerized silica source.

The influence of the ionic strength on the surfactant-silicate assembly process was additionally investigated by performing the synthesis in a reaction solution also containing 1 M NaCl. The presence of the salt leads to a decrease in the regularity of the material, as reflected by the reduction of the number of peaks in the X-ray pattern (from four to two). This effect, expected only at high ionic strengths, is attributed to perturbation of the double layer potential. The strong binding constant of silicate species compared to other ions makes this effect negligible at lower ionic strengths and explains why mesostructure syntheses are relatively insensitive to other counterions in the reaction mixture.

The existence of the cubic mesophase (MCM-48 (ref. 21)) described by Breck *et al.* (2) is strongly supportive of the important role of  $G_{\text{intra}} + G_{\text{inter}}$  in the formation of surfactant-silicate mesostructures. Indeed, there exists remarkable similarity between this cubic mesophase, which we

have recently synthesized and characterized, and the  $Ia\bar{3}d$  phase found in the water-CTABr system (4). A TEM image of the cubic mesostructure material is presented in Figure 6 showing an ordered  $\sim 2000$  Å aggregate. The X-ray powder spectrum in Figure 7 agrees very well with the model  $Q^{230}$  proposed by Mariani *et al.* (22) for water-surfactant systems. For this structure, it is appealing to conjecture that the midplane of the silicate wall sits on a gyroid periodic minimal surface (23). Such a structure can then be viewed as a single infinite silicate sheet separating the surfactant species into two equal and disconnected volumes. This so-called bicontinuous phase will be formed when the optimal head-group area  $A_0$  set by the reaction conditions is close to the value of the  $Ia\bar{3}d$  phase, namely when pH and CTA/SiO<sub>2</sub> ratio are high. It is advantageous for the silicate wall to occupy a periodic minimal surface, because it can maximize the wall thickness for a given CTA/SiO<sub>2</sub> volume fraction.

The leading role of  $G_{intra} + G_{inter}$  in directing mesostructure formation provides a foundation for identifying potential replacement candidates for Si in the synthesis of mesoporous inorganic frameworks. The principal criteria are that the inorganic component must be capable of forming flexible polyionic species, that extensive polymerization of the inorganic component must be possible, and that charge density matching between the surfactant and inorganic species has to occur. In other words, when  $G_{sol}$  plays a benign role,  $G_{wall}$  must not dominate  $G_{intra} + G_{inter}$  for the mesostructure to form. In addition to binding efficiently to the surfactant interface, the best inorganic candidates will have a tendency to form glasses easily. Silicates are certainly a prototypic system due to the ease with which they form oligomeric anions of varying degrees of polymerization. Other systems, however, may also fulfill these requirements, including transition metals, such as vanadium, or main group elements, such as boron, which can form polyanions and condense. One can also speculate about a reversed system in which an anionic surfactant is used to precipitate a cationic metal oxide precursor, the laurylsulfate/iron oxide system representing one candidate example.

Existing experimental data thus far confirm the trends predicted for the formation of surfactant-silicate mesostructures by the qualitative model outlined above. Cooperative binding provides an explanation for the strong interactions needed to precipitate mesophases from low concentration solutions. Preferential polymerization of silicates in the region of the interface, together with a double

layer control of the wall thickness, explains the high regularity of the surfactant-silicate mesostructures. Charge density matching establishes a link between the chemical composition and structure of the silicate wall and the formation of a particular mesostructure. We hope these perspectives will stimulate and guide new experiments aimed at producing and exploiting a better understanding of this exciting new class of materials.

References and notes

1. C. T. Kresge, M. E. Leonowicz, W. J. Roth, J. C. Vartuli, J. S. Beck, *Nature* **359**, 710 (1992).
2. J. S. Beck *et al.*, *J. Am. Chem. Soc.* **114**, 10834 (1992).
3. R. G. Laughlin, *Surfactant Sci. Ser.* **37**, 1 (1991).
4. X. Auvray, C. Petipas, R. Anthore, I. Rico, A. Lattes, *J. Phys. Chem.* **93**, 7458 (1989).
5. The general procedure for synthesizing mesostructure materials is as follows: An aqueous solution containing silica and optional tetramethylammonium hydroxide (TMAOH) is stirred into an aqueous solution containing the surfactant and an optional aluminum source. The resulting mixture is kept at temperatures between 298 and 423 K for reaction times between 5 minutes and 3 days in either closed Teflon bottles, or under stirring and refluxing in a glass flask. For silica sources, we used Cab-O-Sil™ M-5 (Kodak, Rochester, NY), an aqueous solution of sodium silicate (27.5 % SiO<sub>2</sub>, SiO<sub>2</sub>/Na<sub>2</sub>O=3.22 from PQ Corp., Valley Forge, PA), or tetraethylorthosilicate (TEOS) (Aldrich, Milwaukee, WI). Aluminum sources were boehmite (CATAPAL B™ from Alumina Vista, Houston, TX) or sodium aluminate (Spectrum Chemical, Gardena, CA). Quarternary ammonium alkyls C<sub>n</sub>H<sub>2n+1</sub>(CH<sub>3</sub>)<sub>3</sub>NX, X=Cl<sup>-</sup>, Br<sup>-</sup>, and n = 8-18, and tetramethylammonium hydroxide were obtained from Aldrich.
6. The expression "surfactant-silicate" is used here as a comprehensive term for materials synthesized using a mixture of surfactant and silica species, regardless of the particular structure.
7. The transformation between the lamellar and hexagonal mesophases was observed after freeze-drying, as well as air-drying, the filtered samples.
8. Addition of trimethylbenzene (TMB) to the reaction mixture acts to stabilize the lamellar mesophase. Experiments have shown that the 31(±1) Å repeat distance for the layered material shown in Figures 2(A) and 3 is preserved over a range of TMB/surfactant molar

ratios between 0.5-3.0, whereas at lower TMB/surfactant ratios, the hexagonal mesostructure is the favored product. Stabilization of the lamellar mesophase likely occurs because TMB dissolved within the surfactant hydrocarbon assemblies contributes to the hydrophobic chain volume. This increase in surfactant chain volume increases the head-group area  $A_0$  at which the lamellar-to-hexagonal mesophase transformation occurs, according to a simple geometric model (13). Thus, the mesostructural transformation depicted in Figure 2 is a consequence of hydrothermal removal of TMB from within the surfactant chain assembly, combined with an increase of the optimal head-group area  $A_0$ . This is supported by separate experiments which show that addition of TMB to the aqueous phase inhibits the transformation from a lamellar to an hexagonal mesostructure.

9. R. K. Harris, C. T. G. Knight, W. E. Hull, *ACS Symp. Ser.* **134**, 79 (1982); C. T. G. Knight, R. G. Kirkpatrick, E. Oldfield, *J. Mag. Reson.* **78**, (1988); A. V. McCornick and A. T. Bell, *Catal. Rev. Sci. Eng.* **31**, 97 (1989).
10. R. K. Iler, *The Chemistry of Silica* (Wiley, New York, 1979), p. 182.
11. C. J. Brinker, G. W. Scherer, *Sol-Gel Science* (Academic Press, New York, 1990), p. 100.
12. K. Hagakawa, J. C. T. Kwac, *Surfactant Sci. Ser.* **37**, 189 (1991).
13. J. Charvolin and J. F. Sadoc, *J. Phys.* **48**, 1559 (1987); J. N. Israelachvili in *Surfactants in Solution*, p. 3, vol. 4, K. L. Mittal and P. Bothorel, Eds. (Plenum, New York, 1987) proposed the dimensionless parameter  $g=V/A_0l_c$  as a means of determining the preferred configuration of a surfactant assembly, where  $V$  is the volume of the hydrophobic chain and  $l_c$  is the characteristic chain length. According to this treatment, spherical micelles will form if  $g<1/3$ , cylindrical micelles if  $1/3<g<1/2$ , vesicles or bilayers if  $1/2<g<1$ , and inverted micelles if  $g>1$ .
14. As discussed in (8) above, the presence of TMB in the reaction mixture can, but does not always, require a swelling response in surfactant systems.
15. A. Weiss, *Angew. Chem. Int. Ed. Engl.* **20**, 850 (1981).

- 
16. A. Weiss, *Clays and Clay Minerals. Proceedings of the National Conference on Clays and Clay Minerals* (Earl Ingerso, New York, 1961) vol. 10, p. 191.
  17. This is determined from the  $y$ -intercept of a plot of  $d$ -spacings vs. carbon atom number for different chain length surfactants, corrected for the head-group diameter.
  18. Calculated from  $d$ -spacings, volumetric considerations (based on a measured void fraction of 0.65), and from X-ray diffraction refinements using cylinder- and hexagonal-prismatic-rod-packing as models.
  19. A. Monnier and G. D. Stucky, unpublished work.
  20. T. Yanagisawa, T. Shimizu, K. Kuroda, C. Kato, *Bull. Chem. Soc. Jpn.* **63**, 988 (1990).
  21. C. T. Kresge *et al.*, U.S. Patent No. 5,198,203, March 30, 1993.
  22. P. Mariani, V. Luzzati, H. Delacroix, *J. Mol. Biol.* **204**, 165.
  23. A periodic minimal surface is the smallest surface separating a volume into two equal parts, given a certain periodic constraint.
  24. We thank J. Israelachvili, J. Zasadzinski (UCSB), C. T. Kresge, D. Olson, J. Beck, J. Vartuli, and J. Higgins (Mobil) for helpful discussions. This research was funded by the MRL Program of the National Science Foundation under award DMR91-23048, Air Products, du Pont, the Office of Naval Research (G.D.S.), the NSF Science and Technology Center for Quantized Electronic Structures (grant DMR91-20007), the NSF/NYI program and the Camille and Henry Dreyfus Foundation (B.F.C.), and through fellowships by the FNRS (A.M.) and the DFG (F.S.).

## Figure Captions

**Figure 1:** Time evolution of the intensity of X-ray diffraction features associated with layered and hexagonal (M41S) mesostructures at 348 K. The layered material is precipitated rapidly, while the hexagonal material appears later, as a result of a higher degree of silica polymerization. The molar composition of the reaction mixture was 1 SiO<sub>2</sub> : 0.025 Al<sub>2</sub>O<sub>3</sub> : 0.115 Na<sub>2</sub>O : 0.233 CTACl : 0.089 TMAOH : 125 H<sub>2</sub>O.

**Figure 2:** Powder X-ray diffraction patterns of surfactant-silicate mesostructures precipitated from the same reaction mixture (1 SiO<sub>2</sub> : 0.034 Al<sub>2</sub>O<sub>3</sub> : 0.07 Na<sub>2</sub>O : 0.27 CTABr : 0.14 TMAOH : 0.28 TMB : 100 H<sub>2</sub>O), and then treated hydrothermally at T = 373 K for different times. X-ray patterns for (A) the initially precipitated layered material, (B) an intermediate material, and (C) the M41S hexagonal mesostructure acquired zero, one, and ten days, respectively, after initiation of the hydrothermal treatment.

**Figure 3:** Transmission electron micrograph of the layered surfactant-silicate mesostructure whose X-ray data are shown in Figures 1 and 2(A). The *d*-spacing of this material is 31(±1) Å.

**Figure 4:** A schematic diagram of the mechanism proposed for the transformation of a surfactant-silicate system from the lamellar to the hexagonal mesophase. On the left, small silica oligomers (not shown explicitly in the gray SiO<sub>2</sub> region) act as multidentate ligands, which have sufficiently high charge density to permit a lamellar surfactant configuration. As polymerization of the silica proceeds, diminished charge density of larger silica polyanions increases the average head-group area of the surfactant assembly, driving the transformation into the hexagonal mesophase.



A. Monnier *et al.*

**Figure 5:** This chart shows the approximate domains of formation of the lamellar and hexagonal surfactant-silicate mesophases, as functions of pH and silica source. Cab-O-Sil™ is comprised of ca. 100 Å oligomeric silica particles, whereas Na-silicate is a solution of hydrolyzed and essentially monomeric silicates.

**Figure 6:** Transmission electron micrograph of the cubic surfactant-silicate mesostructure showing an ordered ~2000 Å aggregate viewed along its [111] axis.

**Figure 7:** (A) X-ray powder diffraction pattern of the cubic mesostructure, with  $Ia\bar{3}d$  symmetry, synthesized from a reaction mixture with a molar composition of 1 TEOS : 0.25 Na<sub>2</sub>O : 0.65 CTACl : 62 H<sub>2</sub>O for three days at T = 373 K. (B) Calculated diffraction pattern using the Q<sup>230</sup> model proposed by Mariani *et al.* (22) with a lattice parameter  $a = 97.3$  Å.

Figure 1

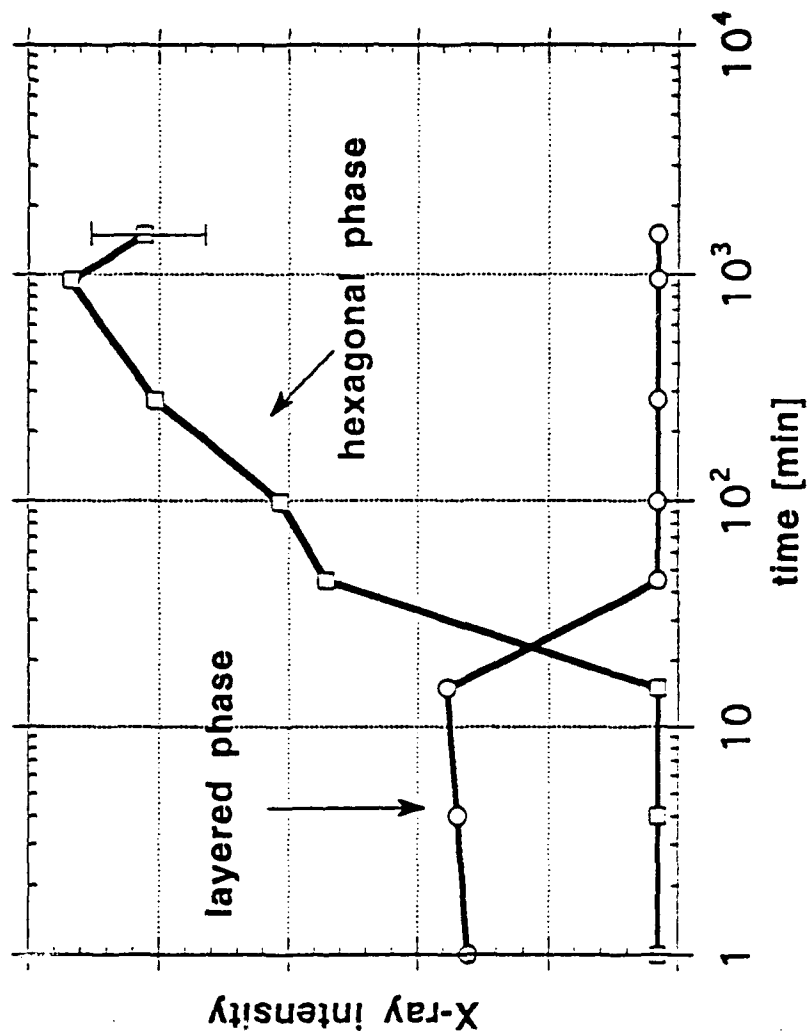


Figure 2

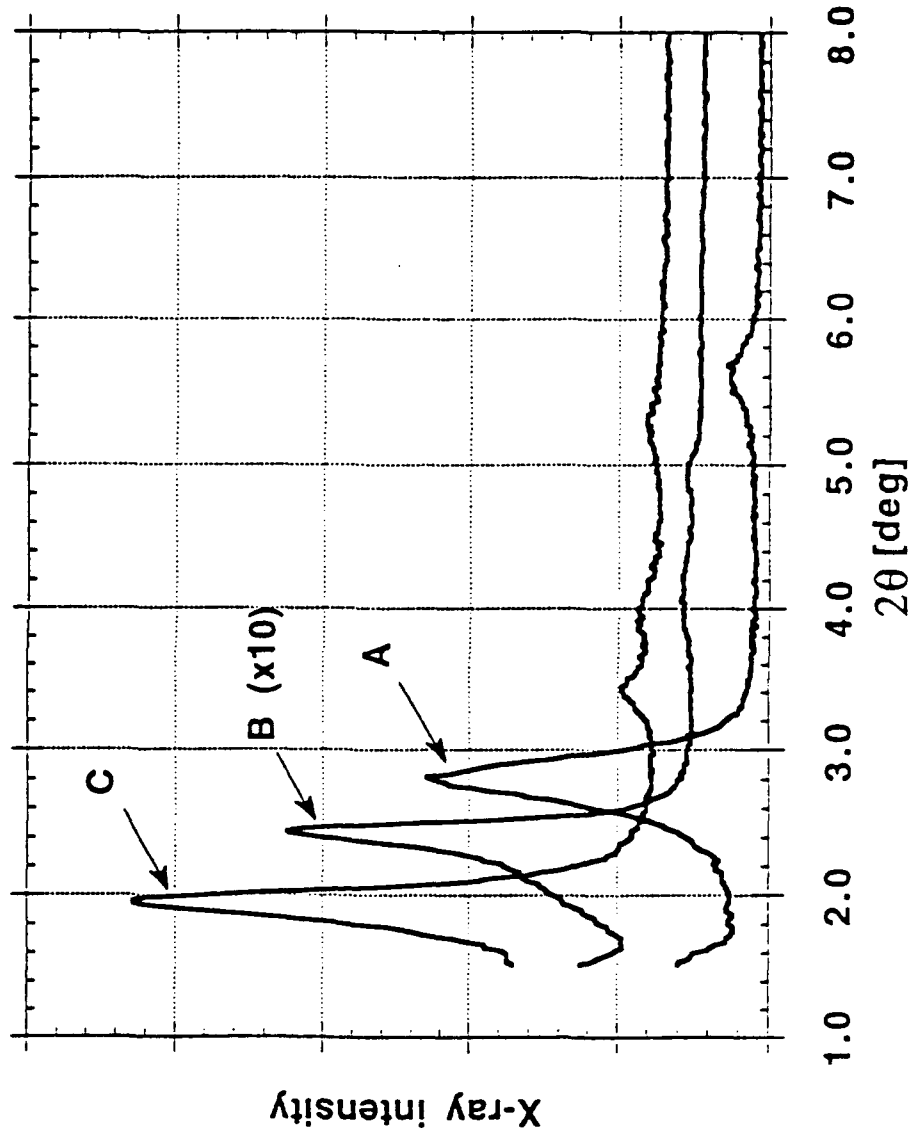


Figure 3

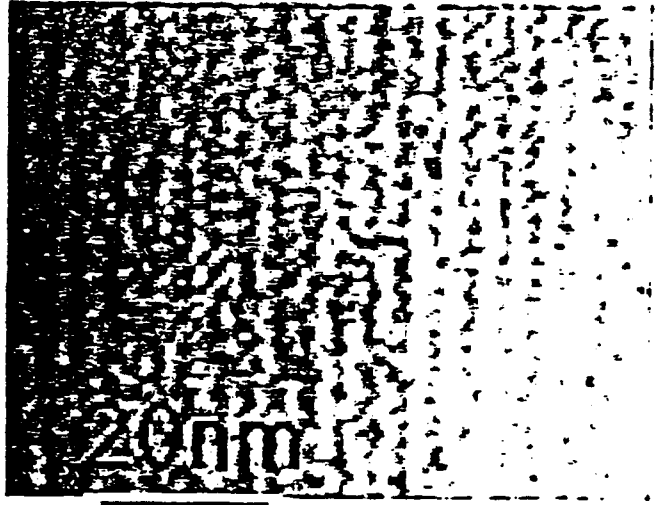
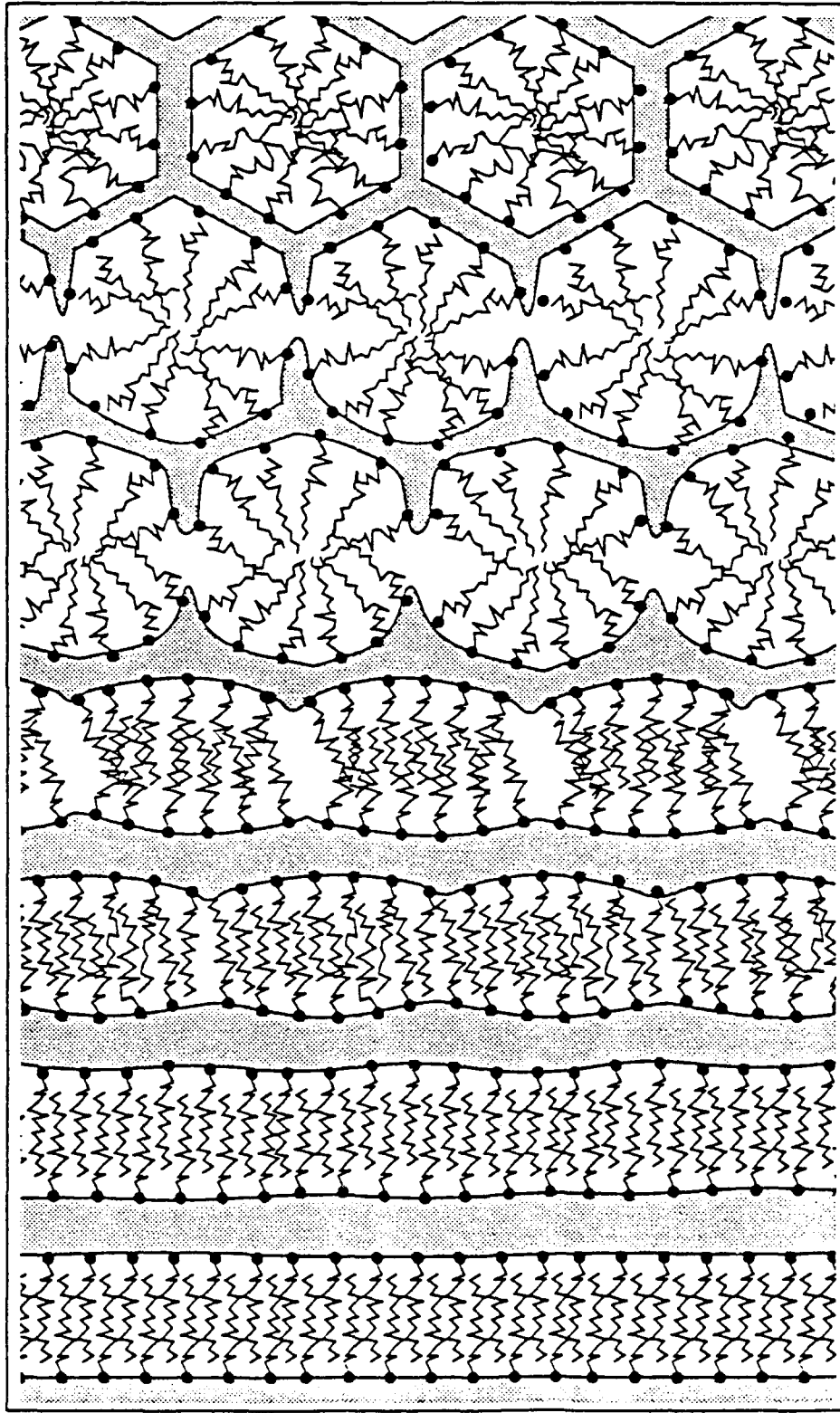


Figure 4



□ SiO<sub>2</sub>    □ Reaction coordinate    ↑

Figure 5

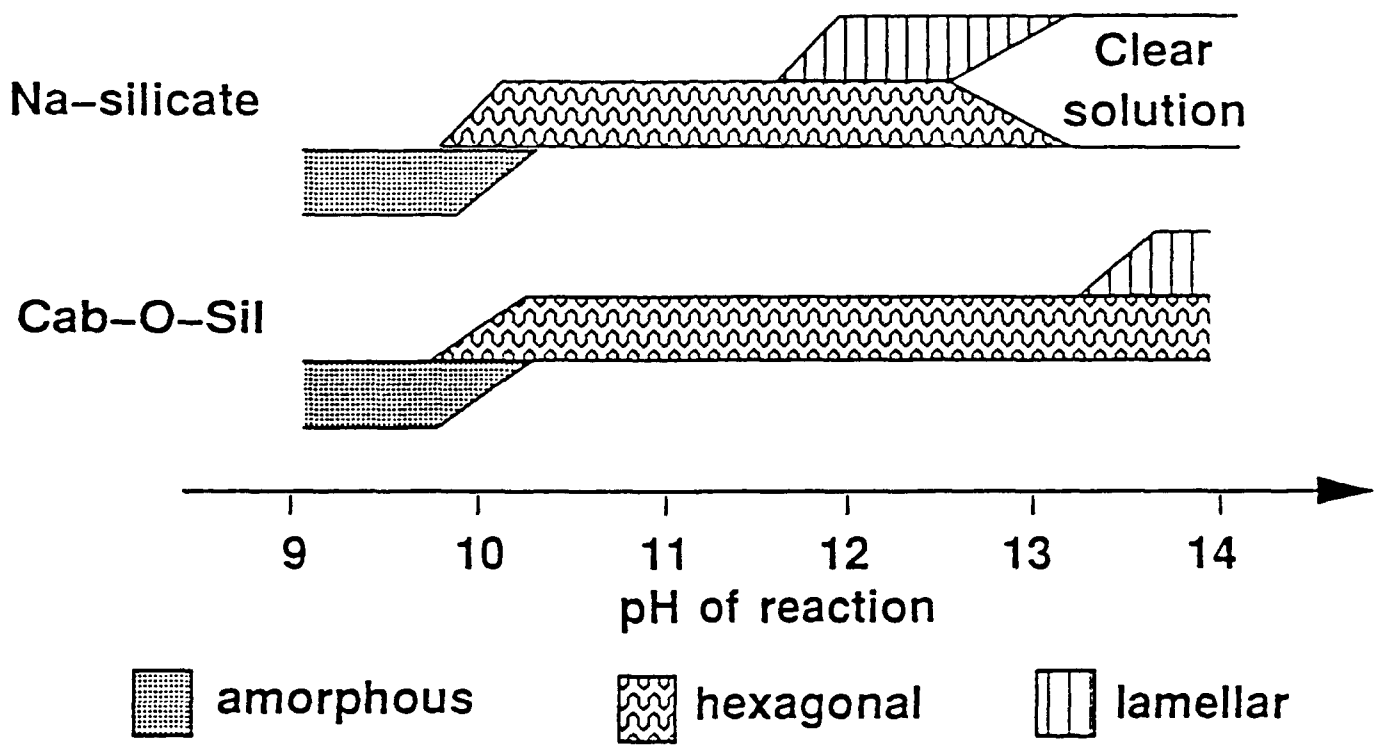


Fig. 6

6

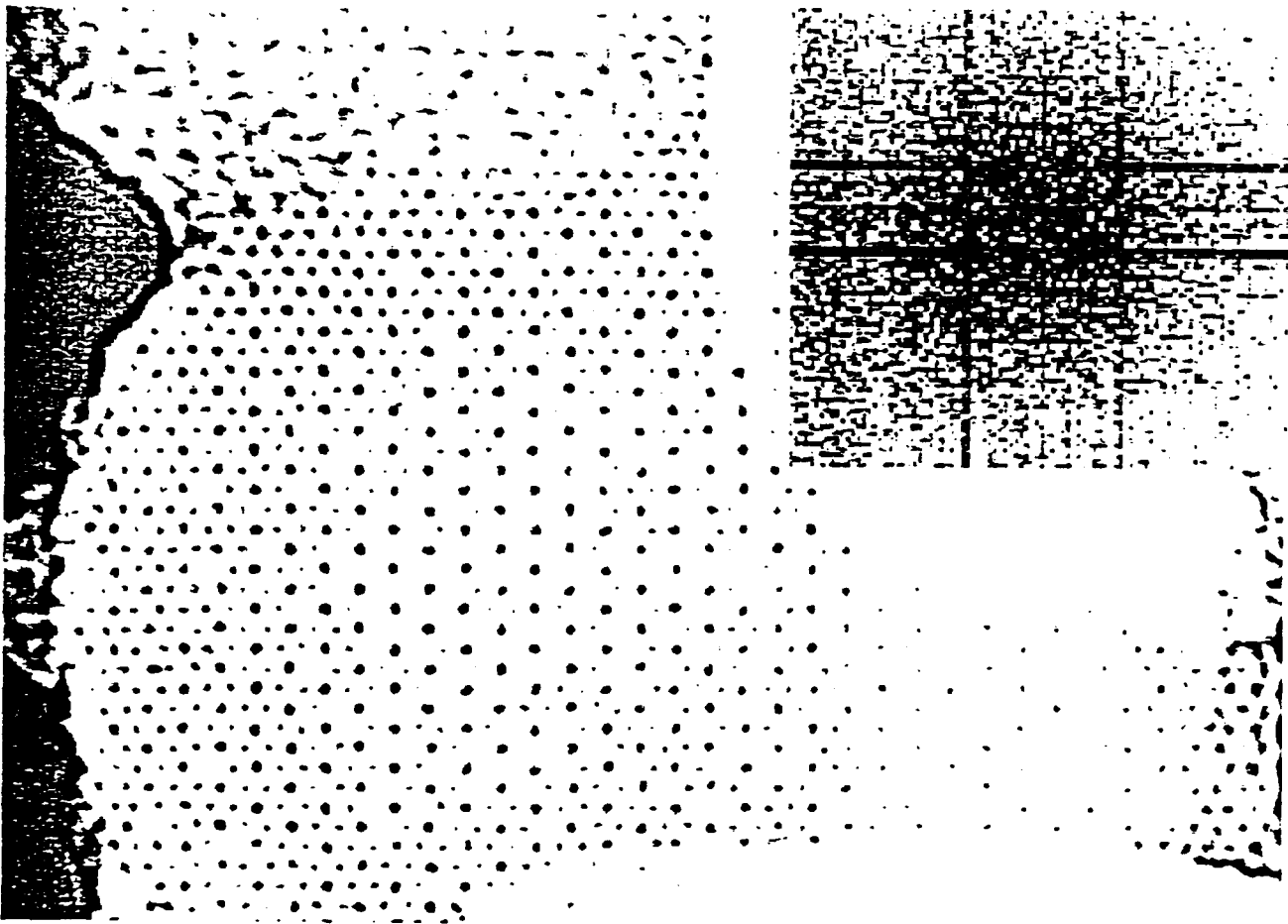
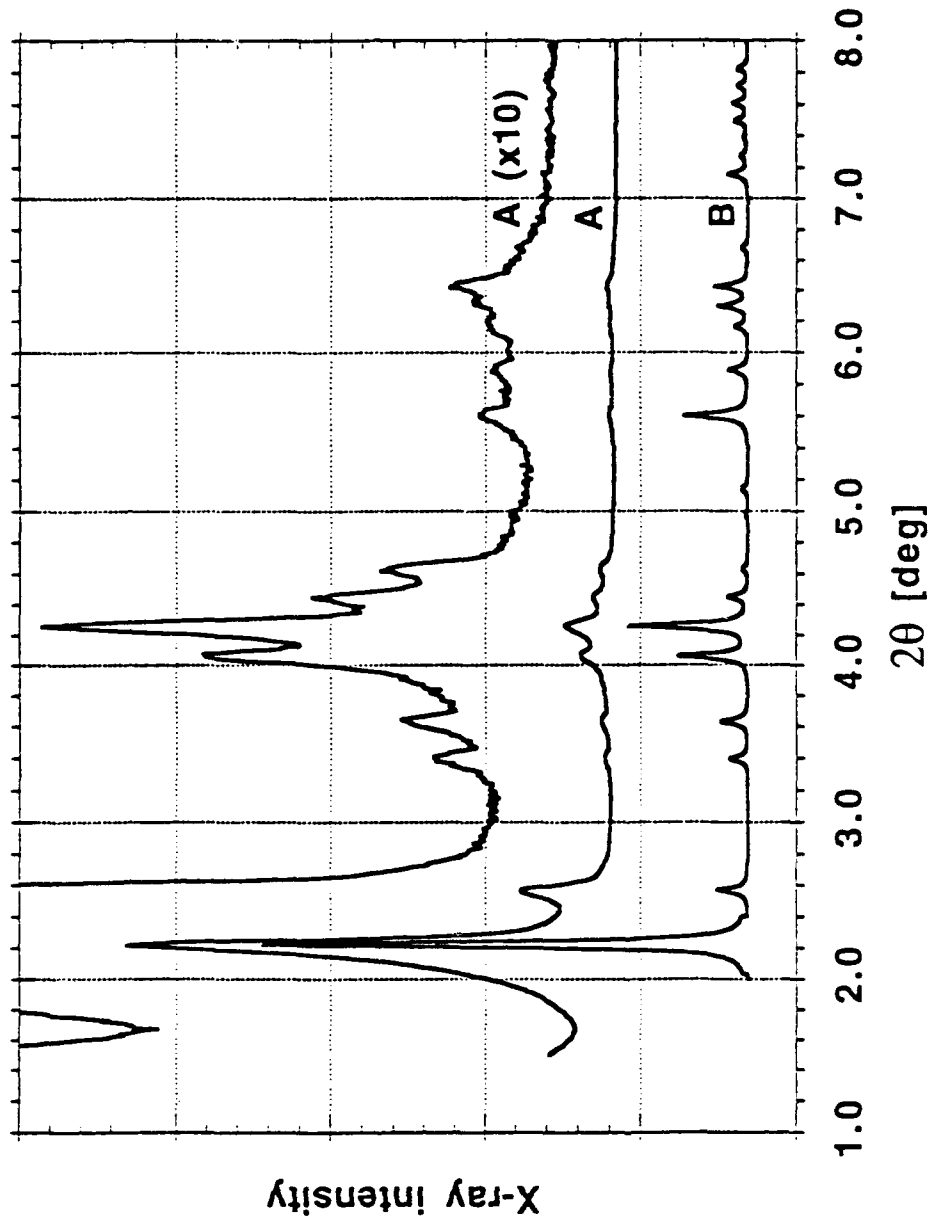


Figure 7





TECHNICAL REPORT DISTRIBUTION LIST - GENERAL

Office of Naval Research (2)\*  
Chemistry Division, Code 1113  
800 North Quincy Street  
Arlington, Virginia 22217-5000

Dr. James S. Murday (1)  
Chemistry Division, Code 6100  
Naval Research Laboratory  
Washington, D.C. 20375-5000

Dr. Robert Green, Director (1)  
Chemistry Division, Code 385  
Naval Air Weapons Center  
Weapons Division  
China Lake, CA 93555-6001

Dr. Elek Lindner (1)  
Naval Command, Control and Ocean  
Surveillance Center  
RDT&E Division  
San Diego, CA 92152-5000

Dr. Bernard E. Douda (1)  
Crane Division  
Naval Surface Warfare Center  
Crane, Indiana 47522-5000

Dr. Richard W. Drisko (1)  
Naval Civil Engineering  
Laboratory  
Code L52  
Port Hueneme, CA 93043

Dr. Harold H. Singerman (1)  
Naval Surface Warfare Center  
Carderock Division Detachment  
Annapolis, MD 21402-1198

Dr. Eugene C. Fischer (1)  
Code 2840  
Naval Surface Warfare Center  
Carderock Division Detachment  
Annapolis, MD 21402-1198

Defense Technical Information  
Center (2)  
Building 5, Cameron Station  
Alexandria, VA 22314

\* Number of copies to forward